processes

MDPI

Article

Energy Optimization and Effective Control of Reactive Distillation Process for the Production of High Purity Biodiesel

Syed Sadiq Ali [1], Agus Arsad [2], SK Safdar Hossain [1], Avijit Basu [1] and Mohammad Asif [3,*]

[1] Department of Chemical Engineering, King Faisal University, P.O. Box 380, Al-Ahsa 31982, Saudi Arabia; ssali@kfu.edu.sa (S.S.A.); snooruddin@kfu.edu.sa (S.S.H.); abasu@kfu.edu.sa (A.B.)
[2] Faculty of Engineering, UTM-MPRC Institute for Oil and Gas, School of Chemical and Energy Engineering, Universiti Teknologi Malaysia, Johor Bahru 81310, Johor, Malaysia; agus@utm.my
[3] Department of Chemical Engineering, King Saud University, P.O. Box 800, Riyadh 11421, Saudi Arabia
* Correspondence: masif@ksu.edu.sa; Tel.: +966-114676849; Fax: +966-114678770

Abstract: Biodiesel is a promising renewable energy option that significantly reduces the emission of greenhouse gases and other toxic byproducts. However, a major challenge in the industrial scale production of biodiesel is the desired product purity. To this end, reactive distillation (RD) processes, which involve simultaneous removal of the byproduct during the transesterification reaction, can drive the equilibrium towards high product yield. In the present study, we first optimized the heat exchange network (HEN) for a high purity RD process leading to a 34% reduction in the overall energy consumption. Further, a robust control scheme is proposed to mitigate any feed disturbance in the process that may compromise the product purity. Three rigorous case studies are performed to investigate the effect of composition control in the cascade with the temperature control of the product composition. The cascade control scheme effectively countered the disturbances and maintained the fatty acid mono-alkyl ester (FAME) purity.

Keywords: biodiesel; reactive distillation; heat integration; process control; optimization

Citation: Ali, S.S.; Arsad, A.; Hossain, S.S.; Basu, A.; Asif, M. Energy Optimization and Effective Control of Reactive Distillation Process for the Production of High Purity Biodiesel. *Processes* **2021**, *9*, 1340. https://doi.org/10.3390/pr9081340

Academic Editor: Chiing-Chang Chen

Received: 1 July 2021
Accepted: 26 July 2021
Published: 30 July 2021

1. Introduction

The continuous depletion of non-renewable energy resources and their hazardous impact on the environment has impelled the scientific community to explore alternative energy sources. Due to consistently increasing energy demands, the need to develop renewable, non-toxic, and environmentally friendly energy options such as biofuels has grown rapidly [1–3].

Biodiesel is similar to petroleum diesel in terms of properties and is a promising alternative to fossil fuels [4–6]. Fatty acid mono-alkyl esters (FAME) are the main component of biodiesel, which can be produced by transesterification of free fatty acids (FFA) and alcohol. The biodegradable feed stocks such as animal fats, vegetables, or cooking oils are common sources of FFA. The optimization and simplification of FFA transformation to the clean-burning biodiesel fuel is a subject of active research [7–10]. While using the conventional reactor-separation system, the reaction equilibrium limits the product yield. The generation of byproducts amplifies the backward reaction, thus limiting the reaction conversion. This limitation instigates the need for multiple separation systems in the process, involving additional capital and operational costs. A potential solution to this drawback is the deployment of a reactive distillation (RD) column. An RD column is a separation column with catalysts in a particular section, which enables the reaction as well as separation to occur simultaneously in the same tray. The RD process is best suited for equilibrium-limited chemical reactions, whereby the byproducts are separated immediately after their formation. This causes the reaction to move forward and results in high conversion and product yield. Additionally, the RD process optimizes the plant economics, eliminating the need for extra separation processes and added utilities [11–15]. Estrada-Villagrana et al. [13] studied

the feasibility of replacing the conventional reactor-separation system with an RD column for the hydrodesulfurization of naphtha. They found that the RD process further reduced the sulfur composition in the product. Moreover, the RD process requires lower capital and operating costs. Saha et al. [16], in his experimental investigation, replaced a conventional batch reactor with RD to produce iso-amyl acetate. This strategy exponentially increased the conversion from 18.2% to 69.5%. Kiss et al. [14] developed an experimental set-up to compare solid acid catalysts for biodiesel production. They further designed an RD process by fitting the same design parameters used for the experimental system. The biodiesel production was enhanced by 6–10 times while the requirement for excess alcohol was reduced. Moreover, the energy consumption and hence the operational costs reduced as well. The cost effective and compact process features of RD makes it well suited for a range of industrial applications from petrochemical industries [13,17] to processes that involve alkylation and acetalization [18–22]. The esterification of FFA is also widely conducted using the RD process to produce biodiesel (FAME) of high composition and yield [23–25].

Various techniques have been proposed to further optimize the RD process in terms of energy efficiency, profitability, and product composition [26–28]. Nguyen and Demirel [29] thermally coupled the RD column with the excess methanol recovery column using the Aspen Plus process simulator. The condenser of the RD column was removed and a portion of the liquid from the recovery column was recycled to the RD column as reflux. The thermal coupling reduced the energy consumptions by 13.1% and 50% in the RD column and the recovery column, respectively. Using dual reactive distillation can significantly increase the conversion and product yield. The addition of heavy alcohol in dual reactive distillation, along with light alcohol participating in the reaction, forms favorable liquid–liquid equilibrium so that all the water can be separated from the RD distillate. Dimian et al. [8] used dual RD columns and reported 100% conversion. The ester product attained 98% purity while the byproduct water was 99.9 mol%. Pérez-Cisneros et al. [30] obtained 99.92 mol% biodiesel and 99.97 mol% byproduct water using integrated dual RD columns in their simulations. Moreover, the researchers have also proposed efficient heat exchange networks for heat integration [23,31]. For example, the heat integrated RD process proposed by Kiss [23] reduced total energy consumption by 45%.

Although a process may remain steady during operation, an unwanted disturbance in any parameter may seriously affect its operation and potentially compromise the product output and composition, and hence limit the process efficiency. Therefore, the design of an efficient process control is required to stabilize the process and maintain the required product quality in case of any disturbance to the process. Additionally, an effective control system ensures process safety, manages environment norms, and reduces operational costs [32]. However, in the current case of an RD process, four components (two reactants and two products) interacting in one system and a limited number of degrees of freedom aggravate the process dynamics [9,28,33,34]. Luyben [35] compared the dynamics of the reactive distillation process with equal feed flow and excess feed flow. The excess feed flow employed an extra separation column to separate excess reactant. The dynamic response was found to be slower due to the recycling and the extra column. However, the excess feed flow process did not require a composition analyzer to monitor the feed, which eliminated the need of an intricate plantwide control scheme. Lee et al. [36] performed the plantwide control design of a reactive distillation column that was thermally coupled with the conventional column. Using one tray temperature control, the product stability was achieved even at high feed flow disturbances. Thus, a carefully designed process control can efficiently stabilize and optimize a complex process such as reactive distillation.

In the present study, an RD process was simulated to produce high purity FAME with an annual production capacity of 12.25 kton and 99.5% purity byproduct water. Dodecanoic acid or lauric acid, which is an FFA, was used as the acid feed, while methanol was used as the alcohol feed in the system. The feed flow rate of methanol was kept at 5% greater than FFA, which required an extra conventional column for excess methanol recovery. Although the equimolar feed flow can preclude the need of this extra column, expensive

and complex operation composition analyzers are required to closely monitor the feed flow rates and composition [35]. Moreover, sensitive flow controllers are required for effective control system since even a slight disturbance may compromise the biodiesel product purity. The aforementioned requirements make the equimolar process infeasible to operate [37]. Therefore, excess reactant is often employed as an alternate to ease RD process control design in the industrial processes [34]. Using excess reactant may increase the capital and operational costs of the process. However, a proper energy management and integrated energy design can cope with the energy requirements and scale down the utilities expenses [8,23]. Another advantage of the proposed process is the high purity water byproduct, which eliminates the need for a water treatment process to conform to environment standards.

Moreover, an optimized heat exchange network was designed using Aspen Energy Analyzer in this study. The proposed heat integrated process is less energy intensive with energy savings of up to 33% compared to the conventional process. In order to consistently manage the product purity, a robust process control structure is an essential requirement. Therefore, a rigorous process control scheme was designed in this study and case studies were undertaken to overcome the impact of disturbances in the process without compromising the product quality. The columns are designed using the Radfrac method in Aspen Plus. The process dynamics and control mechanism were studied using the rigorous pressure driven mode of Aspen Plus.

2. Process Description

2.1. Process Kinetics

FFA reacts with methanol in the liquid phase to produce FAME and water using sulfated zirconia, which is a solid acid catalyst [38]. This esterification reaction can be written as:

$$C_{11}H_{23} - COOH + CH_3 - OH \rightleftharpoons C_{11}H_{23} - COO - CH_3 + H_2O \quad (1)$$

The reaction kinetics of the present esterification reaction are given as:

$$r = k_1 C_{C_{11}H_{23}COOH} C_{CH_3OH} - k_2 C_{C_{11}H_{23}COOCH_3} C_{H_2O} \quad (2)$$

The reaction is reversible, and k_1 and k_2 are reaction constants for forward and backward reactions, respectively. Noting that the byproduct water is continuously extracted from the reaction process, the forward reaction dominates the overall esterification reaction. Since the backward reaction rate is remarkably sluggish, neglecting the backward rate is an acceptable approximation, simplifying the reaction kinetics [23]. Therefore, the reaction kinetics can be expressed as:

$$r = Ae^{\left(\frac{-E_a}{RT}\right)} C_{C_{11}H_{23}COOH} C_{CH_3OH} \quad (3)$$

where A is the Arrhenius factor and E_a is the required activation energy. For the current study [23]:

$$A = 120,000 \ \frac{\mathrm{m}^3}{\mathrm{kmol \cdot s}}; \ E_a = 55,000 \ \frac{\mathrm{J}}{\mathrm{mol}} \quad (4)$$

2.2. VLE Thermodynamics

The multi-component phase equilibrium of the reaction and separation system requires a precise thermodynamic model and relevant parameters. The thermodynamic activity model 'UNIQUAC' is used in the present work for VLE and LLE calculations. The UNIQUAC model is given as [39]:

$$\ln \gamma_i = \ln \frac{\Phi_i}{x_i} + \frac{z}{2} q_i \ln \frac{\theta_i}{\Phi_i} - q_i' \ln t_i' - q_i' \sum_j \frac{\theta_j' \tau_{ij}}{t_j'} + l_i + q_i' - \frac{\Phi_i}{x_i} \sum_j x_j l_j \quad (5)$$

The binary interaction parameters used in the activity model are listed in Table 1. The binary parameters were deduced experimentally [37], whilst the FFA-FAME and methanol–water parameters can be extracted from Aspen properties. The components in the system can be arranged in the following order in terms of their volatility:

$$\alpha_{Methanol} > \alpha_{Water} > \alpha_{FAME} > \alpha_{FFA} \quad (6)$$

Table 1. Binary parameters of UNIQUAC activity model.

Comp. i	Acid	Methanol	Methanol	Methanol	Acid	Water
Comp. j	FAME	Water	Acid	FAME	Water	FAME
A_{ij} **(K)**	0	−1.0662	0	0	−0.29924	0
A_{ji} **(K)**	0	0.6437	0	0	−0.38437	0
B_{ij} **(K^2)**	238.8469	432.8785	48.3493	31.789	−195.44	−216.733
B_{ji} **(K^2)**	−369.561	−322.1312	−309.554	−539.979	−107.62	−658.816

The light key component recovered in the RD distillate is water along with excess methanol while the heavy key in the bottom is FAME with traces of FFA. The residue curve for methanol/water/FAME system at 9 bar (RD operating pressure) is reported in Figure 1a. The separation of high purity FAME is feasible, however high heat duty is required. The separation of methanol and water is performed in the conventional column. The T-xy diagram at an operating pressure of 5 bar is plotted in Figure 1b.

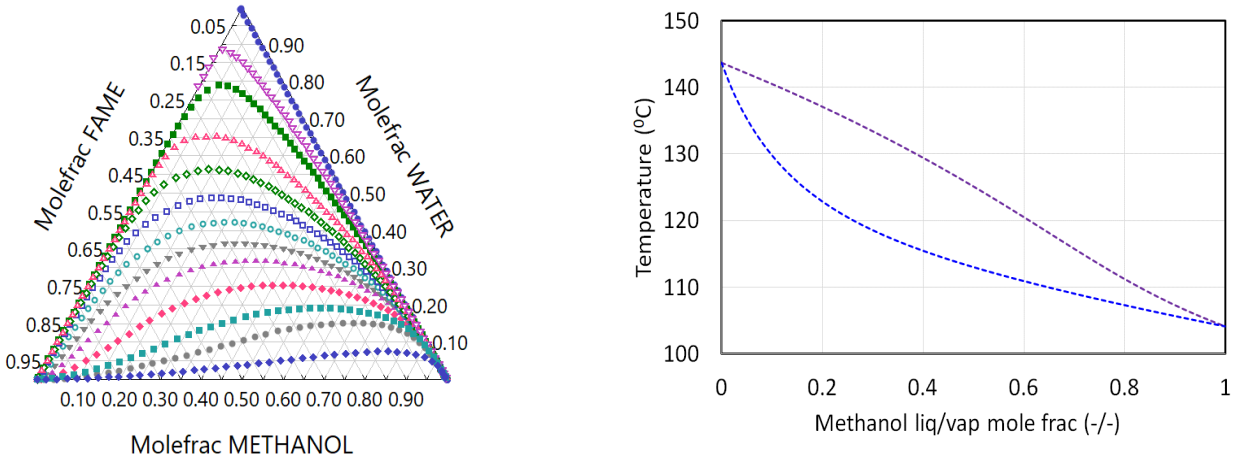

(**a**) (**b**)

Figure 1. Thermodynamic relations. (**a**) Residue curve for FAME–Methanol–Water. (**b**) T-xy diagram for methanol–water.

The following assumptions were made in the present simulation:

- The liquid and vapor in all the trays are completely mixed
- Both the liquid and vapor streams leaving the tray are in equilibrium.
- The vapor hold-up in the tray is negligible
- The liquid phase is homogenous in all trays.

2.3. Steady State RD Process

The process flowsheet is shown in Figure 2 and the important design parameters, reported by Ali et al. [40], are used to simulate the process. The design parameters are reported in Table 2. The tray numbers in both columns are denoted from top to bottom so that the first tray represents the condenser and the last tray is the reboiler. The methanol and

FFA with 100% purity at ambient temperature are used as reactants. The fresh methanol blends with recycled methanol and enters the RD column with FFA in stages 15 and 6, respectively, after preheating to the desired temperature. The liquid hold-up is set at 50 L so that flooding from the trays can be avoided. The RD column produces 99.5 mol% FAME as bottoms, while the distillate comprises of unreacted methanol and water. The stream results of the process are mentioned in Table 3. The excess methanol and water exiting from RD distillate is separated in the conventional distillation column (CC). The water purity is maintained at 99.5% in the CC bottom. The methanol–water mixture recovered from the CC top with a high concentration of methanol is recycled back and mixed with the fresh methanol feed. The first column, i.e., the RD column shown in Figure 3, involves the production of FAME and water from methanol and FFA in the reaction section and the simultaneous transfer of water from the liquid phase to the vapor phase providing an added advantage. The liquid phase and vapor phase compositions in the trays are reported in Figure 4. In the stripping section, below the reaction section, the FAME in the vapor phase moving upwards is transferred to the liquid phase further enhancing the FAME concentration in the liquid phase below. The lighter components are transferred from vapor to liquid coming downstream from the condenser as reflux in the enriching section. In order to reduce the recycling load and achieve a steady state, a 10% effluent is purged out from the recycling process using a splitter, which is 0.57 kmol/h with a methanol/water ratio of 0.47/0.53, respectively. The purge constitutes only 4.6% of the total feed input supplied in the process. The purge effluent can be used in the process, which requires dilute methanol [41]. Moreover, the purge comprises only 5 mol% of the total water produced in the process and 4.2 mol% of the total methanol fed into the system.

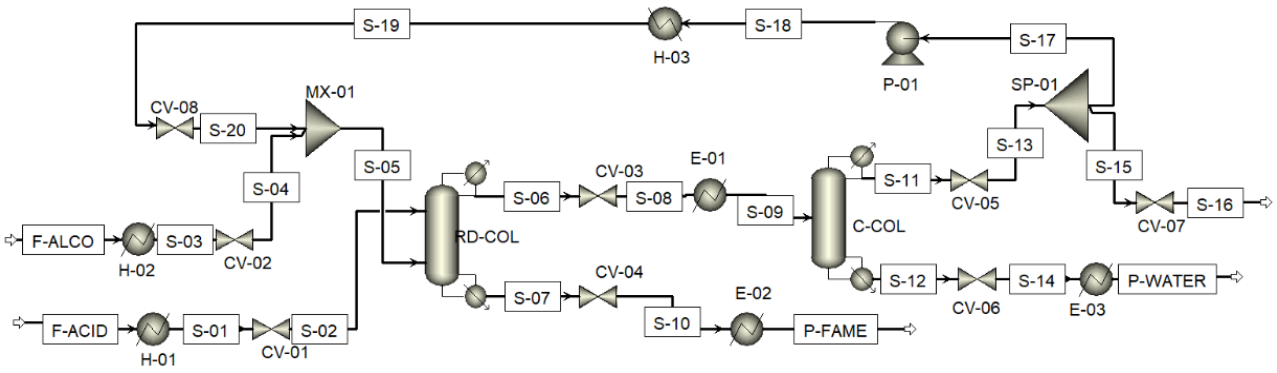

Figure 2. Process flowsheet for the production of high purity biodiesel.

Table 2. Process design parameters of distillation columns.

	RD Column	Column 2
Number of stages	18	10
Feed stage	Above 6 and 16	7
Reactive stages	6–15	-
Operating pressure	9 bar	5 bar
Reflux ratio	0.8	3
Reboiler duty	360 kW	258.2 kW
Condenser duty	−208.5 kW	−234.8 kW
Reactive stages liquid hold-up	50 L	-

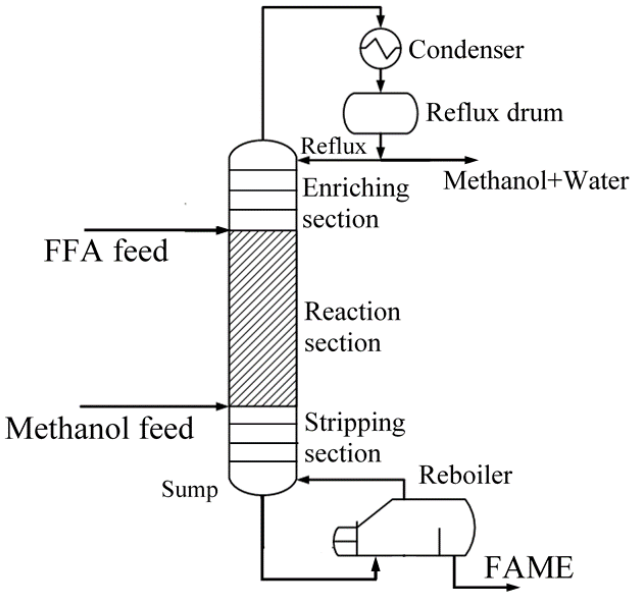

Figure 3. Detailed schematic of RD process.

Table 3. Stream results of the biodiesel process.

Stream Name	F-ACID	F-ALCO	S-05	P-FAME	P-WATER	S-16
Temperature (°C)	25	25	150	375.9	144.22	114.16
Pressure (bar)	13.03	13.1	9.1	4.1	2.06	1.0
Vapor Fraction	0	0	1	0	0	0
Mole Flows (kmol/h)	6	6.3	9.84	6.03	5.69	0.57
Mole Fractions (-/-)						
ACID	1	0	0	0.0006	0.000	0.000
FAME	0	0	0	0.9945	0.000	0.000
METHANOL	0	1	0.92	0	0.0048	0.47
WATER	0	0	0.08	0.0049	0.9952	0.53

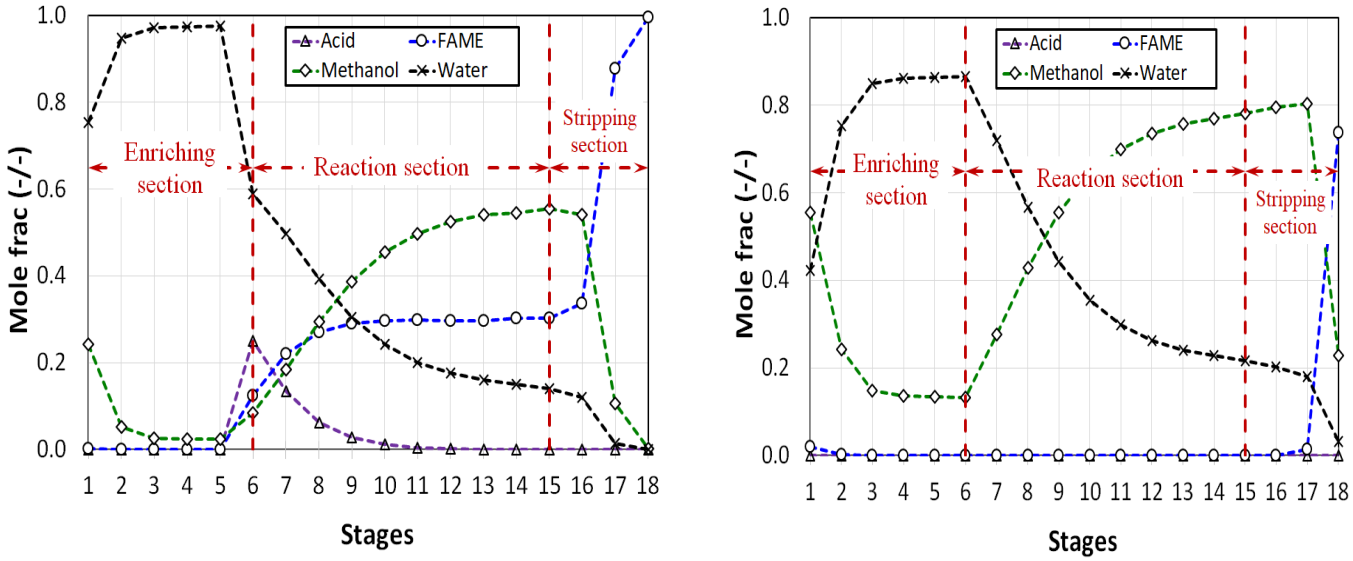

Figure 4. Stage composition profile of RD-column. (**a**) Liquid phase. (**b**) Vapor phase.

3. Results and Discussion

3.1. Heat Integration

The heat integration parameters of the streams of the process flowsheet in Figure 2, which require heating and cooling and are included in the optimized heat exchange design, are reported in Table 4. The majority of utilities required are for the preheating of reactants, whereby the utilities can be efficiently replaced by the hot process effluents, which must be cooled before their utilization. The cold utilities requirement is lessened as well. The modified heat exchange network (HEN) of the process is reported in Figure 5. There are five new heat exchangers, which replaced the process heaters and coolers in Figure 2. Since the condensers and reboilers of the distillation columns involve phase changes and require equilibrium conditions, the heat integration design becomes a complicated task. For example, the kettle type exchangers generally used for reboilers involve vapor and liquid separation as well. Moreover, there are high possibilities of involvement of multiple heat exchangers for single reboiling/condensing processes since the enthalpy of one stream may not be enough to maintain equilibrium and achieve the required process conditions. Moreover, distillation columns in some cases have condensing and reboiling processes inside the column integrated with sump or the surge tank. Therefore, the condensers and reboilers of columns are not accounted for in the heat exchange network in the present modified HEN. Table 5 compares the various economic parameters of the preliminary process reported in Figure 2 and heat integrated process reported in Figure 5. The requirement of both hot and cold utilities was reduced by 22.7% and 24.8%, respectively. Other miscellaneous energy savings, such as electricity, contributed to a further reduction. Therefore, the overall energy consumption was reduced by 33.6% while the estimated capital cost remained the same in both cases. Moreover, the temperature interval diagram plotted in Figure 6 shows that the stream S-15, which is the bottom stream from the RD column reboiler, has a temperature of around 366 °C, while the cold streams have to be heated to a maximum of 150 °C. The heaters and coolers drawn here refer to PFD in Figure 2. The minimum approach temperature is set at 10 °C. The heat available in section A in the TID diagram is the excess energy available after designing the HEN, which is removed in E-01 in Figure 5. The 140.12 kW of energy available at 366 °C can be used for preheating streams that require heating up to high temperatures, which is an added advantage of the heat integration of the process.

Table 4. Stream conditions of the process flowsheet reported in Figure 2 used for heat integration.

Streams	Condition	T_{in} (°C)	T_{out} (°C)	$Q_{available}$ (kW)
F-ALCO	Cold	25	150	−76.2
F-ACID	Cold	25	150	−99.1
S-08	Hot	150	50	26.6
S-10	Hot	358.4	25	333.8
S-14	Hot	144.2	25	16.2
S-18	Cold	115.7	150	−35.3

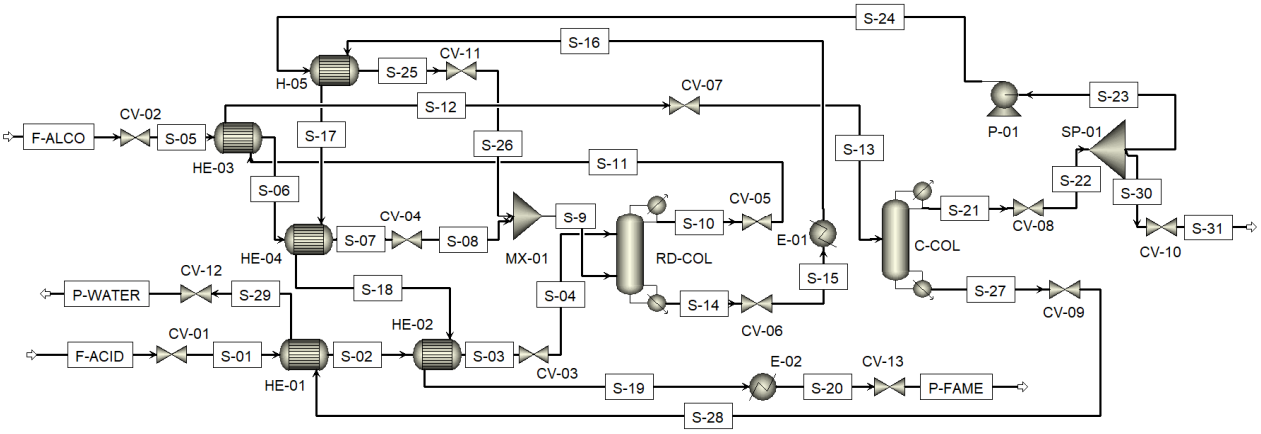

Figure 5. Heat integrated process flowsheet for the production of high purity biodiesel.

Table 5. Total costs and utilities required in the biodiesel production process.

	Process without Heat Integration	Heat Integrated Process
Capital cost (USD)	5,910,470	5,901,860
Annual utility cost (USD)	173,599	115,256
Total hot utilities (kW)	799.5	618.2
Total cold utilities (kW)	−801.1	−602.5
Energy savings	-	33.6%

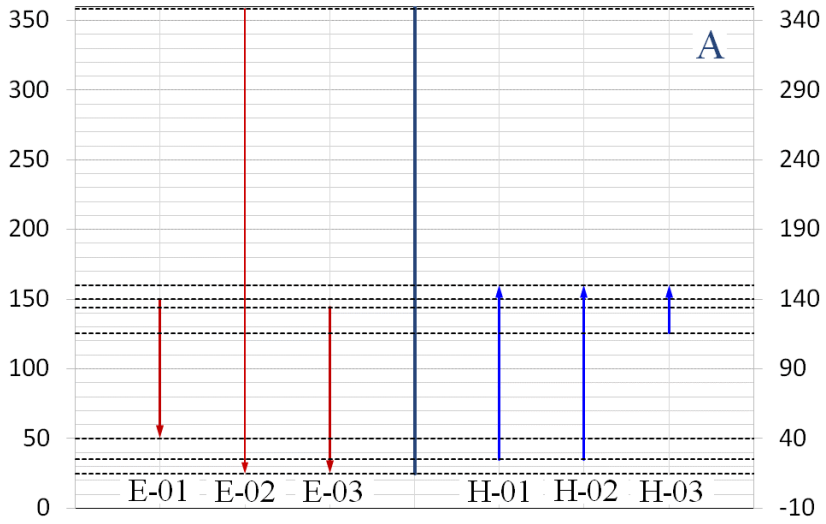

Figure 6. Temperature interval diagram.

3.2. Process Control Structure

In the current process control structure, the objective is to maintain the purity of the product, FAME, and the other effluent from the distillation column, water, if any changes occur in the feed flow rates. The rigorous plantwide control process suggested by Luyben is used in the current study [34]. There are a total of 11 controllers used for controlling the process. The following control loops were added to the process:

Level controllers (LC): Since the surge/storage tanks have a flexible range of variation and do not require stringent control, proportional controllers were installed as level controllers to maintain liquid level at reflux drum and sump of the reactive distillation column and the distillation column.

Flow controllers (FC): The equi-molar feed flow in the process employs composition analyzers and flowmeters with high precision and sensitivity, which are expensive and involve strenuous operation. Any stoichiometric misproportion may result in process dynamics instability and require complex process control arrangements to be enacted in such situations. Adding one reactant in excess in the process eliminates the equal feed flow requirement and hence the complex measurement devises. However, the excess reactant has to be separated from the feed, which employs an extra distillation column.

The PI controllers were set to control the feed flow rates in the column. The fresh methanol feed flow, along with recycled methanol, was controlled before entering the column. A ratio controller is attached to maintain the methanol feed flow with respect to acetic acid in the column at a fixed ratio at any time.

Pressure controllers (PC): In order to maintain the condenser pressure in both columns, PI controllers are installed in both columns. The heat removal from the condenser was manipulated by controlling the coolant flow in the condenser.

Temperature controllers (TC): The temperature controller was installed to control the temperature of trays in the column. The process output was the heat duty of the reboiler. The PI controllers were installed as temperature controllers in both columns. A dead time of 1 min was used with temperature controllers.

Composition controller (CC): The composition controller is used in Case 4 below to effectively manage the product purity of the reactive distillation column. Since the response of cascade controller is sluggish, a dead time of 3 min is used with the control scheme.

The tuning parameters of FC, PC, and LC were taken from the standard tuning parameters suggested by Luyben [42], while the tuning parameters for TC and CC controllers were calculated from the Ziegler-Nichols tuning method [32]. The details and tuning parameters used for controllers are reported in Table 6.

The following case studies were performed in the current study:

3.2.1. Case I

This case study was performed without using feed flow ratio control and composition control structures. As seen in Figure 7, a total of ten control loops were installed. The control scheme faceplates of all the controllers are reported in Figure 8. Although the composition control was not used, the temperature controller installed in both columns can manage the tray temperatures as well as composition to an extent. A dead time of 1 min is added to the control structure. Figure 9a shows the response of effluents when the methanol feed flow was increased from 6.3 kmol/h to 6.6 kmol/h at time 2 h. The FAME product increased from 6 kmol/h to 6.1 kmol/h, since the reaction shifted towards product side due to the increase in reactant, methanol. Moreover, the RD distillate flow (Stream S-10) increased due to excess methanol (0.2 kmol/h increase) and excess water produced (0.1 kmol/h) due to increased reactivity. However, the water in CC bottom decreased and the CC distillate flow increased (Stream S-21), and hence the effluent in the recycling process as well as columns increased. When the methanol increased in the CC column, there was a higher transfer of methanol from liquid to vapor in the stripping section, which increased the total vapor flow rate and reduced the liquid flow rate in the reboiler, which in turn resulted in lower CC bottom flow rate, which is water. Moreover, the increased vapor flow after cooling in

a condenser resulted in higher amounts of distillate. Although there was slight increase in FAME concentration, the concentration of water decreased slightly due to increased methanol in the CC column. Additionally, it took 2.5 h for FAME concentration to stabilize. Henceforth, the methanol feed flow was decreased from 6.3 kmol/h to 6.0 kmol/h. The disturbance effects are reported in Figure 9b. It should be noted that the methanol feed flow is equivalent to acid feed flow. A decrease in FAME product is seen since the reaction is shifted towards the reactant side. The water product increased due to the decrease in methanol in the CC column feed flow. The FAME concentration decreased while the water concentration increased. The time taken for stable FAME concentration is approximately 2.5 h here as well.

Table 6. Controller details and tuning parameters.

Controller ID	Controller Type	Controlled Variable	Manipulated Variable	Tuning Parameters
FC-01	PI	Acid feed flow	Acid feed flow	$K_C = 0.5$ $\tau_I = 0.3$
FC-02	PI	Methanol feed flow	Methanol feed flow	$K_C = 0.5$ $\tau_I = 0.3$
LC-RD-C	P-only	RD-reflux drum level	RD-distillate flow	$K_C = 2$
LC-RD-B	P-only	RD-sump level	RD-bottom flow	$K_C = 2$
LC-CC-C	P-only	CC-reflux drum level	CC-distillate flow	$K_C = 2$
LC-CC-B	P-only	CC-sump level	CC-bottom flow	$K_C = 2$
PC-RD	PI	RD-condenser pressure	RD-condenser duty	$K_C = 20$ $\tau_I = 12$
PC-CC	PI	CC-condenser pressure	CC-condenser duty	$K_C = 20$ $\tau_I = 12$
TC-RD	PI	RD-tray 17 temperature	RD-reboiler duty	$K_C = 1.98$ $\tau_I = 11.5$
TC-CC	PI	CC-tray 9 temperature	CC-reboiler duty	$K_C = 2$ $\tau_I = 10$
CC-RD	PI	RD-bottom composition	RD-TC set point	$K_C = 1.1$ $\tau_I = 27.5$

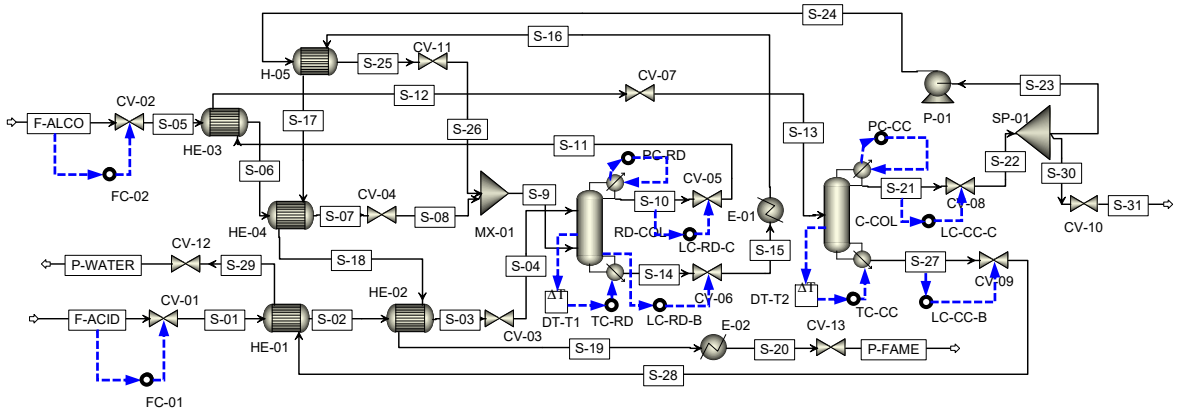

Figure 7. Process flow diagram with control scheme used in Case I (composition control and feed ratio control not included).

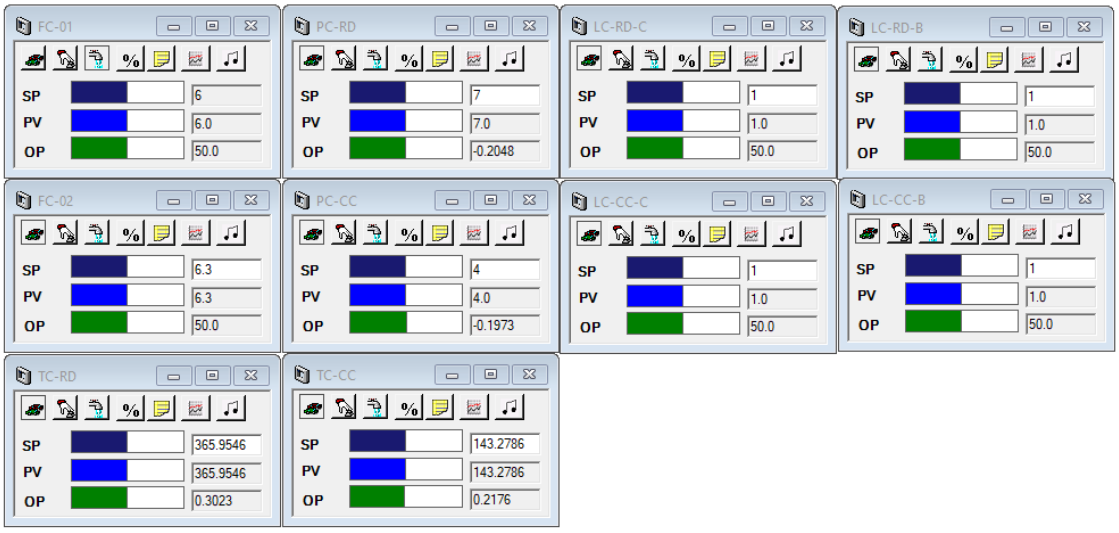

Figure 8. Control scheme faceplates of the process.

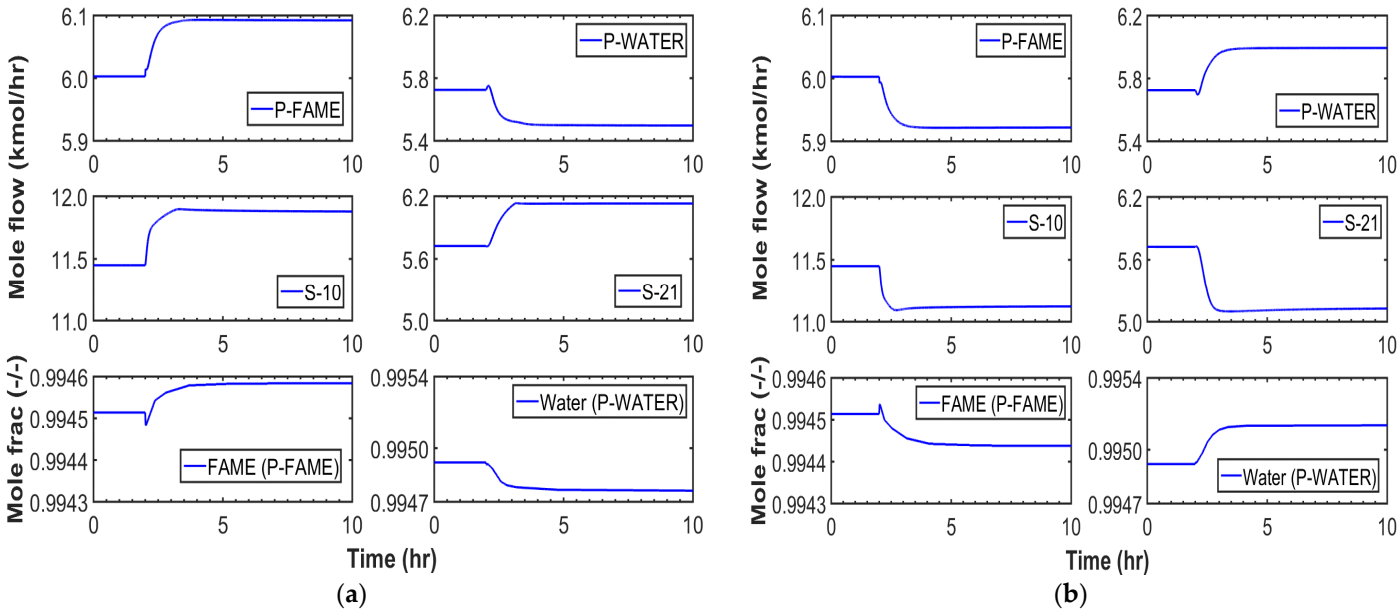

Figure 9. Stream results when the methanol feed flow was changed; (**a**) +5% change; (**b**) −5% change.

3.2.2. Case II

In this case study, a feed flow ratio control was added, as seen in Figure 10 (without composition control, but with temperature control in the RD column). The ratio control ensures that one feed flow rate remains in proportion with the other feed flow. In the present study, the acid feed flow is at a ratio of 1.0/1.05 (kmol/h basis) to methanol flow feed. The first graph in Figure 11 shows that the acid feed flow immediately changes from 6 kmol/h to 6.29 kmol/h when the methanol feed flow is changed from 6.3 kmol/h to 6.6 kmol/h. It should be noted that the ratio control will be enacted only in the case of methanol feed flow disturbances. The FAME product flow increased due to the increase in reactants. However, the effluent in the process has increased (Stream S-10 and S-21). A marginal decrease in mole fractions of products is seen due to higher unreacted reactants in the product streams. The FAME composition became steady after more than 2 h.

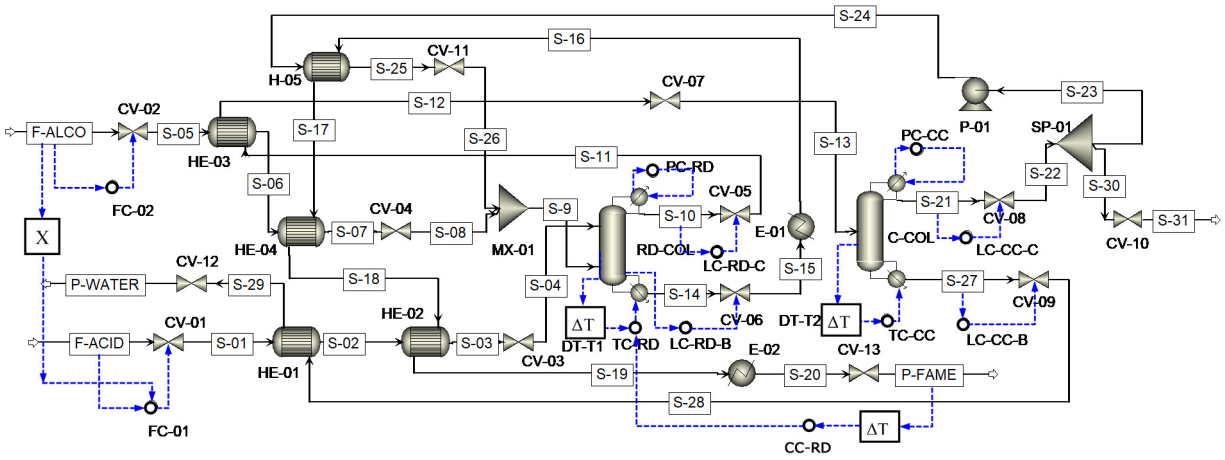

Figure 10. Process flow diagram with control scheme including composition control and feed ratio control used in Cases II and III.

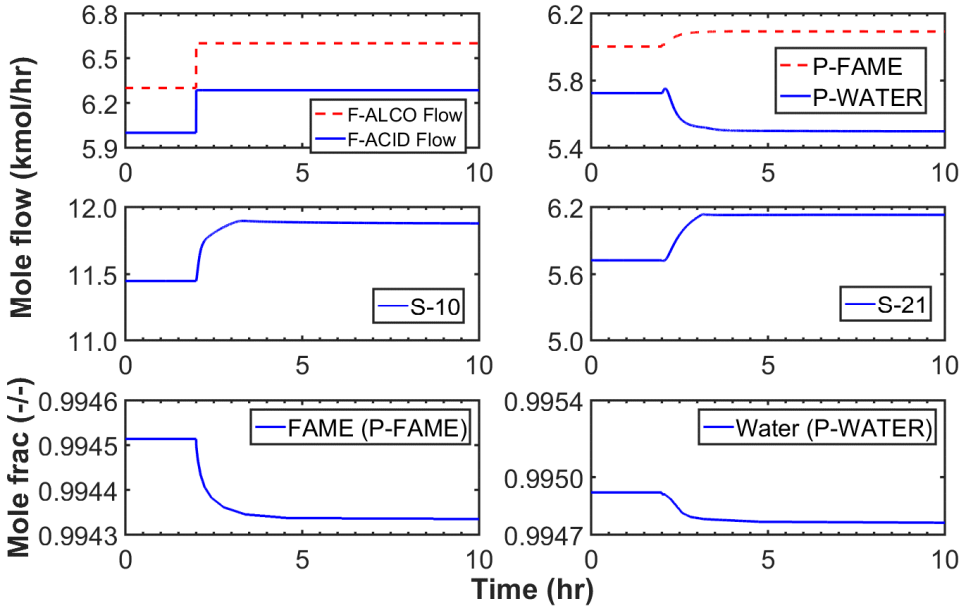

Figure 11. Stream results without cascade control scheme when the methanol feed flow was changed by +5%.

3.2.3. Case III

The operation with temperature controller may sometimes generate an offset in the product composition, which can be subsided using a composition controller. However, the CC control generates a delayed response, which can again compromise the composition quality. Hence, the control scheme is used in a cascade loop with a temperature controller. The control loop structure is reported in Figure 10 and the cascade control arrangement faceplate is reported in Figure 12. The temperature control scheme acts as a primary loop, while the composition control scheme is set as a secondary loop. The process output of the composition controller, which is temperature, is synchronized as the set point of the primary controller. It can be clearly seen in Figure 13 that the composition of the FAME product is almost invariant with the change in reactants feed flow, providing a steady product quality irrespective of the disturbances in the process.

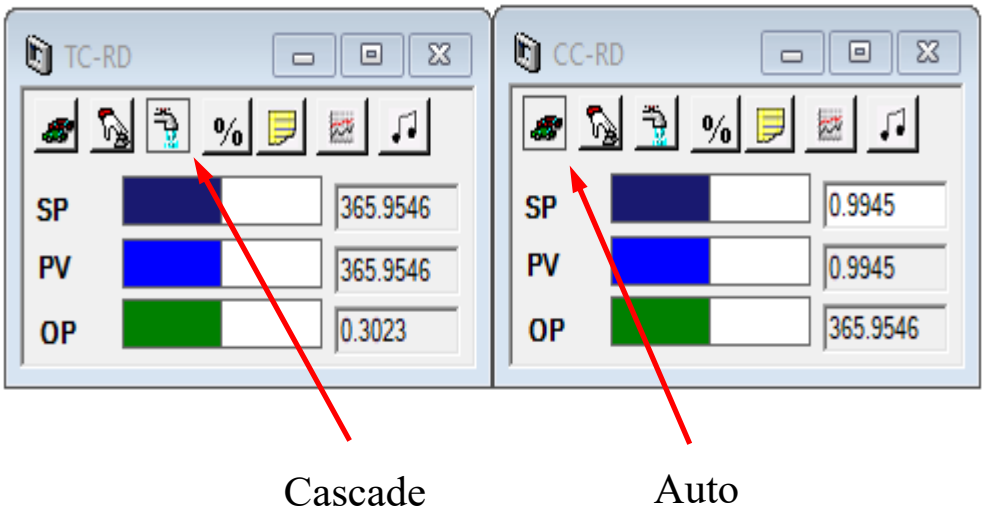

Figure 12. Cascade control scheme faceplates of the process.

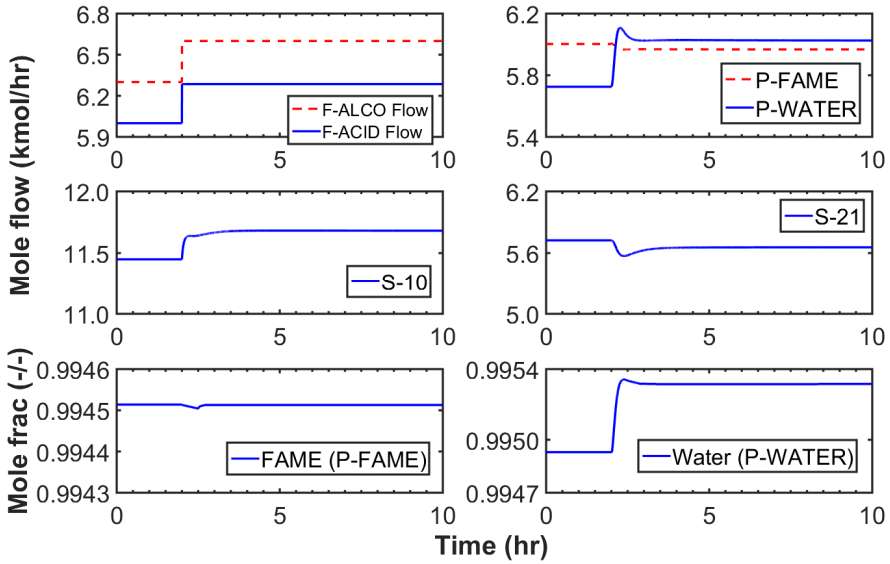

Figure 13. Stream results with cascade control scheme when the methanol feed flow was changed by +5%.

4. Conclusions

Incorporating excess methanol in the proposed flowsheet, although it required an extra distillation column, successfully circumvented the need for a complex process design, complicated control, and expensive compound composition analyzers. The process flowsheet, designed using the design parameters of the previous study [40], produced 99.5 mol% FAME and 99.5 mol% byproduct water. A 10% recycle methanol was purged to reduce the recycle load and improve the water purity. The optimized modified HEN proposed here significantly reduced the cold and hot utilities by decreasing the utility costs by 33.6%.

In the first case study, ±5% change in the methanol feed flow affected both products' flow and composition. The FAME composition was, however, stabilized after 2.5 h of disturbance. A ratio control used in the second case ensured the flow of both feeds at a fixed ratio. This strategy helped to better control the FAME composition. The third case study employed a composition control along with feed ratio control. The operation of composition control in cascade with the temperature control system successfully mitigated

the product composition variations in case of any disturbances in the methanol feed flow rate.

Author Contributions: Conceptualization, Methodology, Software, Validation, Original draft preparation, S.S.A.; Writing, Review, Editing, A.A., S.S.H. and A.B.; Supervision, Final draft preparation, M.A. All authors have read and agreed to the published version of the manuscript.

Funding: This research was funded by the Deanship of Scientific Research, King Faisal University, K.S.A., through Nasher Research Project No. 216012.

Institutional Review Board Statement: Not Applicable.

Informed Consent Statement: Not Applicable.

Data Availability Statement: Not Applicable.

Acknowledgments: The authors are grateful to the Deanship of Scientific Research at King Faisal University for supporting and funding this work through Nasher Research project no. 216012.

Conflicts of Interest: The authors declare no conflict of interest.

References

1. Veljković, V.B.; Biberdžić, M.O.; Banković-Ilić, I.B.; Djalović, I.G.; Tasić, M.B.; Nježić, Z.B.; Stamenković, O.S. Biodiesel production from corn oil: A review. *Renew. Sustain. Energy Rev.* **2018**, *91*, 531–548. [CrossRef]
2. Thangaraj, B.; Solomon, P.R.; Muniyandi, B.; Ranganathan, S.; Lin, L. Catalysis in biodiesel production—A review. *Clean Energy* **2018**, *3*, 2–23. [CrossRef]
3. Pasha, M.K.; Dai, L.; Liu, D.; Guo, M.; Du, W. An overview to process design, simulation and sustainability evaluation of biodiesel production. *Biotechnol. Biofuels* **2021**, *14*, 129. [CrossRef] [PubMed]
4. Atadashi, I.M.; Aroua, M.K.; Aziz, A.A. Biodiesel separation and purification: A review. *Renew. Energy* **2011**, *36*, 437–443. [CrossRef]
5. Patel, A.D.; Zabeti, M.; Seshan, K.; Patel, M.K. Comparative Technical Process and Product Assessment of Catalytic and Thermal Pyrolysis of Lignocellulosic Biomass. *Processes* **2020**, *8*, 1600. [CrossRef]
6. Chozhavendhan, S.; Vijay Pradhap Singh, M.; Fransila, B.; Praveen Kumar, R.; Karthiga Devi, G. A review on influencing parameters of biodiesel production and purification processes. *Curr. Res. Green Sustain. Chem.* **2020**, *1–2*, 1–6. [CrossRef]
7. Castro, F.I.G.; Ramirez, V.R.; Hernandez, J.G.S.; Castro, S.H.; El-Halwagi, M.M. Simulation study on biodiesel production by reactive distillation with methanol at high pressure and temperature: Impact on costs and pollutant emissions. *Comput. Chem. Eng.* **2013**, *52*, 204–215. [CrossRef]
8. Dimian, A.C.; Bildea, C.S.; Omota, F.; Kiss, A.A. Innovative process for fatty acid esters by dual reactive distillation. *Comput. Chem. Eng.* **2009**, *33*, 743–750. [CrossRef]
9. Bildea, C.S.; Kiss, A.A. Dynamics and control of a biodiesel process by reactive absorption. *Chem. Eng. Res. Des.* **2011**, *89*, 187–196. [CrossRef]
10. Abomohra, A.E.-F.; Elsayed, M.; Esakkimuthu, S.; El-Sheekh, M.; Hanelt, D. Potential of fat, oil and grease (FOG) for biodiesel production: A critical review on the recent progress and future perspectives. *Prog. Energy Combust. Sci.* **2020**, *81*, 100868. [CrossRef]
11. Vargas, E.C.; Hernandez, S.; Hernandez, J.G.S.; Rodriguez, M.I.C. Simulation study of the production of biodiesel using feedstock mixtures of fatty acids in complex reactive distillation columns. *Energy* **2011**, *36*, 6289–6297. [CrossRef]
12. Šulgan, B.; Labovský, J.; Labovská, Z. Multi-Aspect Comparison of Ethyl Acetate Production Pathways: Reactive Distillation Process Integration and Intensification via Mechanical and Chemical Approach. *Processes* **2020**, *8*, 1618. [CrossRef]
13. Estrada-Villagrana, A.D.; Quiroz-Sosa, G.B.; Jiménez-Alarcón, M.L.; Alemán-Vázquez, L.O.; Cano-Domínguez, J.L. Comparison between a conventional process and reactive distillation for naphtha hydrodesulfurization. *Chem. Eng. Process. Process Intensif.* **2006**, *45*, 1036–1040. [CrossRef]
14. Kiss, A.A.; Omota, F.; Dimian, A.C.; Rothenberg, G. The heterogeneous advantage: Biodiesel by catalytic reactive distillation. *Top. Catal.* **2006**, *40*, 141–150. [CrossRef]
15. Segovia-Hernández, J.G.; Hernández, S.; Bonilla Petriciolet, A. Reactive distillation: A review of optimal design using deterministic and stochastic techniques. *Chem. Eng. Process. Process Intensif.* **2015**, *97*, 134–143. [CrossRef]
16. Saha, B.; Teo, H.; Alqahtani, A. iso-Amyl Acetate Synthesis by Catalytic Distillation. *Int. J. Chem. React. Eng.* **2005**, *3*, A11. [CrossRef]
17. Al-Arfaj, M.A.; Luyben, W.L. Plantwide control for TAME production using reactive distillation. *AIChE J.* **2004**, *50*, 1462–1473. [CrossRef]
18. Ali, S.S.; Hossain, S.S.; Asif, M. Dynamic modeling of the isoamyl acetate reactive distillation process. *Pol. J. Chem. Technol.* **2017**, *19*, 59. [CrossRef]

19. Hasabnis, A.; Mahajani, S. Acetalization of Glycerol with Formaldehyde by Reactive Distillation. *Ind. Eng. Chem. Res.* **2014**, *53*, 12279–12287. [CrossRef]
20. Guo, B.; Li, Y. Analysis and simulation of reactive distillation for gasoline alkylation desulfurization. *Chem. Eng. Sci.* **2012**, *72*, 115–125. [CrossRef]
21. Yamaki, T.; Matsuda, K.; Na-Ranong, D.; Matsumoto, H. Intensification of Reactive Distillation for TAME Synthesis Based on the Analysis of Multiple Steady-State Conditions. *Processes* **2018**, *6*, 241. [CrossRef]
22. Wei, H.-Y.; Rokhmah, A.; Handogo, R.; Chien, I.L. Design and control of reactive-distillation process for the production of diethyl carbonate via two consecutive trans-esterification reactions. *J. Process Control* **2011**, *21*, 1193–1207. [CrossRef]
23. Kiss, A.A. Heat-integrated reactive distillation process for synthesis of fatty esters. *Fuel Process. Technol.* **2011**, *92*, 1288–1296. [CrossRef]
24. Agarwal, M.; Singh, K.; Chaurasia, S.P. Simulation and sensitivity analysis for biodiesel production in a reactive distillation column. *Pol. J. Chem. Technol.* **2012**, *14*, 59. [CrossRef]
25. Kianimanesh, H.R.; Abbaspour-Aghdam, F.; Derakhshan, M.V. Biodiesel production from vegetable oil: Process design, evaluation and optimization. *Pol. J. Chem. Technol.* **2017**, *19*, 49. [CrossRef]
26. Li, J.; Zhou, H.; Sun, L.; Zhang, N. Design and control of different pressure thermally coupled reactive distillation for synthesis of isoamyl acetate. *Chem. Eng. Process. Process Intensif.* **2019**, *139*, 51–67. [CrossRef]
27. Zhao, T.; Li, J.; Zhou, H.; Ma, Z.; Sun, L. A thermally coupled reactive distillation process to intensify the synthesis of isopropyl acetate. *Chem. Eng. Process. Process Intensif.* **2018**, *124*, 97–108. [CrossRef]
28. Kiss, A.A.; Bildea, C.S. Integrated reactive absorption process for synthesis of fatty esters. *Bioresour. Technol.* **2011**, *102*, 490–498. [CrossRef]
29. Nguyen, N.; Demirel, Y. Using thermally coupled reactive distillation columns in biodiesel production. *Energy* **2011**, *36*, 4838–4847. [CrossRef]
30. Pérez-Cisneros, E.S.; Mena-Espino, X.; Rodríguez-López, V.; Sales-Cruz, M.; Viveros-García, T.; Lobo-Oehmichen, R. An integrated reactive distillation process for biodiesel production. *Comput. Chem. Eng.* **2016**, *91*, 233–246. [CrossRef]
31. Poddar, T.; Jagannath, A.; Almansoori, A. Use of reactive distillation in biodiesel production: A simulation-based comparison of energy requirements and profitability indicators. *Appl. Energy* **2017**, *185*, 985–997. [CrossRef]
32. Seborg, D.E.; Edgar, T.F.; Mellichamp, D.A.; Doyle, F.J.D., III. *Process Dynamics and Control*, 4th ed.; John Wiley and Sons: Hoboken, NJ, USA, 2016.
33. Hung, S.-B.; Chen, J.-H.; Lin, Y.-D.; Huang, H.-P.; Lee, M.-J.; Ward, J.D.; Yu, C.-C. Control of plantwide reactive distillation processes: Hydrolysis, transesterification and two-stage esterification. *J. Taiwan Inst. Chem. Eng.* **2010**, *41*, 382–402. [CrossRef]
34. Luyben, W.L.; Yu, C.C. *Reactive Distillation Design and Control*, 1st ed.; John Wiley & Sons: Hoboken, NJ, USA, 2008. [CrossRef]
35. Luyben, W.L. Economic and Dynamic Impact of the Use of Excess Reactant in Reactive Distillation Systems. *Ind. Eng. Chem. Res.* **2000**, *39*, 2935–2946. [CrossRef]
36. Lee, H.-Y.; Lai, I.K.; Huang, H.-P.; Chien, I.L. Design and Control of Thermally Coupled Reactive Distillation for the Production of Isopropyl Acetate. *Ind. Eng. Chem. Res.* **2012**, *51*, 11753–11763. [CrossRef]
37. Omota, F.; Dimian, A.C.; Bliek, A. Fatty acid esterification by reactive distillation. Part 1: Equilibrium-based design. *Chem. Eng. Sci.* **2003**, *58*, 3159–3174. [CrossRef]
38. Kiss, A.A.; Dimian, A.C.; Rothenberg, G. Biodiesel by Catalytic Reactive Distillation Powered by Metal Oxides. *Energy Fuels* **2008**, *22*, 598–604. [CrossRef]
39. Elliott, J.R.; Lira, C.T. *Introductory Chemical Engineering Thermodynamics*, 2nd ed.; Prentice Hall: Hoboken NJ, USA, 2012.
40. Ali, S.S.; Asif, M.; Basu, A. Design and simulation of high purity biodiesel reactive distillation process. *Pol. J. Chem. Technol.* **2019**, *21*, 1–7. [CrossRef]
41. Simon Araya, S.; Liso, V.; Cui, X.; Li, N.; Zhu, J.; Sahlin, S.L.; Jensen, S.H.; Nielsen, M.P.; Kær, S.K. A Review of The Methanol Economy: The Fuel Cell Route. *Energies* **2020**, *13*, 596. [CrossRef]
42. Luyben, W.L. *Distillation Design and Control Using Aspen Simulation*, 2nd ed.; John Wiley and Sons: Hoboken, NJ, USA, 2013.